Hindawi
Complexity
Volume 2024, Article ID 2333859, 14 pages
https://doi.org/10.1155/2024/2333859

Research Article

Stability Evaluation of Slope Based on Global Sensitivity Analysis

Zhaoxia Xu,[1,2,3] **Xiuzhen Wang**,[1,4] **Lu Guo**,[1] **and Teng Yu**[1,3]

[1]*School of Civil Engineering and Architecture, Suqian University, Suqian 223800, China*
[2]*School of Civil Engineering, Chongqing University, Chongqing 400045, China*
[3]*Key Laboratory of Geological Environment and Engineering Health Monitoring, Suqian University, Suqian 223800, China*
[4]*Jiangsu Prefabricated Building and Intelligent Construction Engineering Research Center, Suqian University, Suqian 223800, China*

Correspondence should be addressed to Xiuzhen Wang; wangxiuzhen@vip.qq.com

Received 7 December 2023; Revised 28 January 2024; Accepted 25 April 2024; Published 21 May 2024

Academic Editor: Qingling Wang

The uncertainty of parameters will have a significant impact on slope stability, where sensitivity analysis is a commonly used method in uncertainty research. However, traditional sensitivity analysis method costs much computation time. When calculating the sensitivity index of one parameter, all other parameters are taken as fixed values, and the uncertainty of all parameters cannot be considered simultaneously. Therefore, the variance-based and the moment-independent global sensitivity analysis (GSA) methods are both introduced to determine the influence of geotechnical parameters on slope stability in this study. To solve the importance index of GSA, the least angle regression algorithm, the kernel density estimation, and orthogonal polynomial estimation methods are developed to obtain variance-based importance index and the moment-independent importance index, respectively. The proposed methods allow all variables to change simultaneously within their variation range and have high computational efficiency. The results are in good at with those obtained by the variance-based Monte Carlo simulation method, which is considered as the exact solution forobtaining the importance index. The influence of the correlation between the shear strength parameters (c and φ) on the importance index is also studied, which indicates that the negative correlation will have a great impact on the importance index, which in turn affects the safety assessment of slope. Three engineering cases have been studied for engineering application, and the compared results indicate that the impact of the geotechnical parameters uncertainty on the safety factor (Fs) and failure probability (p_f) are different. Therefore, the approaches based on GSA which can integrate the Fs with p_f will be a promising approach for slope stability evaluation.

1. Introduction

It is well-known that the uncertainty of random variables will greatly affect the output response. It is important for engineering risk assessment to determine the influence of the uncertainty of random variables on output response [1]. There are many uncertainties in the actual slope engineering, so it is important to study these uncertainties for slope stability. For example, Cai et al. [2] proposed an adaptive sampling method based on limit equilibrium model and stochastic condition method in slope stability analysis to reduce the uncertainty. In order to determine the availability of qualitative and quantitative methods for uncertainty analysis in rock slope stability, Abdulai and Sharifzadeh [3] analyzed and summarized the uncertainty and uncertainty analysis methods, problems, and development in geotechnical engineering modeling. Zhao and Li [4] used artificial bee colony and relevance vector machine to establish a model to describe the relationship between displacement increments and geomechanical parameters so as to predict rock mass deformation and related uncertainties. Under the combined action of continuous rainfall and water level fluctuation, Su et al. [5] studied the stability of reservoir slope using the deterministic method and uncertain method (the Monte Carlo simulation method). It is worth noting that although there are many studies focusing on the uncertainty of geological parameters, while the sensitivity analysis method costs much computation time. When calculating the sensitivity index of one parameter, all other parameters are taken as fixed values, and the uncertainty of all parameters cannot be considered simultaneously. Further research is needed to quantify and distinguish the impact of this uncertainty on the slope stability [6, 7].

Sensitivity analysis is a commonly used method in uncertainty research, and the global sensitivity analysis (GSA) method has got more and more attention in recent years. GSA, also known as importance measurement analysis, considers changes in geotechnical parameters simultaneously and allows them to change over their entire range of distribution (i.e., uncertainty range). According to the importance index of each variable, the relatively important and unimportant parameters can be distinguished, and the relative contribution of the uncertainty of each random variable to the uncertainty of the model output response can be quantified. In slope engineering activities, focusing on the uncertainty of parameters with high importance index can greatly reduce the uncertainty of output response, thus effectively improving the efficiency of slope engineering design and optimization.

Among the global sensitivity analysis methods, the variance-based method and the moment-independent method are widely used, and the first method is usually considered to be an exact solution, which is often used to verify other methods. A large amount of literature has conducted in-depth research on these two methods. For example, Alexanderian et al. [8] developed a variance-based sensitivity analysis method that uses the correlation structure of the problem under study and uses alternative models to speed up the calculation. Subramanian and Mahadevan [9] proposed a semianalytical method based on variance-based sensitivity analysis for calculating the sensitivity index of linear systems with Gaussian random process inputs and nonlinear systems with non-Gaussian random process outputs. Yun et al. [10] proposed a new method to calculate moment-independent importance index based on the law of total expectation in the successive intervals without overlapping and Bayes theorem. Xu et al. [11] proposed a moment-independent method combined with the kernel density estimate to analysis the uncertainty of the geotechnical parameters for slope stability. Khan et al. [12] proposed and tested a method for accelerating global sensitivity analysis in the context of free-form shape optimization.

Therefore, considering the uncertainty of the impact factor of the slope stability, the variance-based global sensitivity analysis method combined with the least angle regression algorithm and the moment-independent global sensitivity analysis method combined with kernel density estimation and orthogonal polynomial estimation are developed to determine the influence of the uncertainty of the influence parameters of slope stability.

2. Methods of the Global Sensitivity Analysis

2.1. Least Angle Regression (LARS) Algorithm. The essence of GSA of geotechnical parameters in slope stability is data mining, and feature selection techniques can be used to evaluate the importance of these parameters under a certain standard. Among feature selection methods, supervised feature selection algorithms have been increasingly used, such as the forward selection algorithm and the forward gradient algorithm. Combining the advantages of the forward selection algorithm and the forward gradient algorithm, Efron et al. [13] proposed the LARS algorithm. LARS improves the disadvantage that the forward gradient algorithm only advances a small step in each fitting and regression process and improves the operation efficiency. However, its step size is less than the step size of the forward selection algorithm to ensure the accuracy of the results.

The main operation process of LARS algorithm is as follows: first, all the coefficients in the regression model are set to 0, and the input variable with the greatest correlation with the output response is found. Second, find a second input variable in the direction of this input variable that maximizes the correlation coefficient with the current residual vector. Finally, follow the direction of the angle bisector of the abovementioned two input variables to find the third variable in the same way, and so on until all input variables are selected into the regression model or reach the set threshold, and finally, all regression coefficient vectors and predicted value are obtained. The predicted value of the response can be obtained by the LARS algorithm in n steps (n represents the number of input variables), which is much smaller than the forward gradient algorithm (it needs thousands of steps). Therefore, the computational efficiency has been significantly improved. The regression model of the LARS algorithm can be expressed as follows [14]:

$$\min S(\widehat{\beta}) = \|y - \widehat{\mu}\| = \sum_{i=1}^{n} (y_i - \widehat{\mu}_i)^2 = \sum_{i=1}^{n} \left(y_i - \sum_{j=1}^{m} x_{ij}\beta_j \right)^2, \quad (1)$$

where $(x_{i1}, x_{i1}, \cdots, x_{im})$ and y_i are the input variables and output response corresponding to the i^{th} sample, respectively; $\widehat{\mu}_i$ is the predictive value of the output response; and β_j is the regression coefficient of x_{ij}. To make $S(\widehat{\beta})$ reach the minimum value, it is necessary to continuously adjust β_j through the LARS algorithm, and the following conditions are met:

$$\sum_{j=1}^{m} \left|\beta_j\right| \leq t_c, \quad (2)$$

where t_c is the constraint value, and $t_c \geq 0$.

Then, the variance-based importance measure index S_i can be expressed as follows:

$$S_i = \frac{\mathrm{Var}(\widehat{Y})}{\mathrm{Var}(Y)} \tag{3}$$

where $i = 1, 2, \cdots, n$, and $\mathrm{Var}(Y)$ and $\mathrm{Var}(\widehat{Y})$ are expressed as follows, respectively:

$$\mathrm{Var}(Y) = \frac{1}{N-1}\sum_{k=1}^{N}\left(y_k - \overline{y}\right)^2, \tag{4}$$

$$\mathrm{Var}(\widehat{Y}) = \frac{1}{N-1}\sum_{k=1}^{N}\left(\widehat{\mu}_k - \overline{\widehat{\mu}}_k\right)^2, \tag{5}$$

where $\overline{y}$ is the mean of the output response Y, $\widehat{\mu}_k$ is the predictive value, which can be obtained by LARS, and $\overline{\widehat{\mu}}_k$ is the mean value of $\widehat{\mu}_k$.

According to the abovementioned principles, the function of Y needs to run N times to obtain the importance index, where N is the sample size of the random variables.

S_i obtained by Monte Carlo simulation is considered to be an exact solution and is usually used to verify the results of other methods in the global sensitivity analysis. Therefore, S_i was used for the comparative analysis in this study, which is expressed as follows [15]:

$$S_i^v = \frac{\mathrm{Var}\left(E\left(Y\middle|x_i\right)\right)}{\mathrm{Var}(Y)}, \tag{6}$$

where $E(Y|x_i)$ is the conditional mean value of Y.

It is well-known that the function of Y needs to run $(nN+1)N$ times to obtain the importance index, where n is the number of the random variables, and N is the same as abovementioned.

2.2. Moment-Independent Method. It is pointed out that the variance-based GSA method only considers variance, and S_i will inevitably lead to the loss of parameter information and lack of moment independence. In view of this, Borgonovo [16] proposed a moment-independent importance index based on the comprehensive consideration of the requirements of Satelli, Helton, and Davis for the importance index (i.e., globality, universality, quantification, and moment independence). The principle of moment-independent method is to study the average influence of the uncertainty of the input parameters on the probability density function or cumulative distribution function of the model output response, so as to determine the influence of the input parameters on the output response. It can obtain a global estimate of the importance of the input parameters in the model, and its computational efficiency is much higher than that of variance-based GSA methods.

The process of the moment-independent method is as follows: Substitute the random variables $X_1, X_2, \cdots, X_n$ into the function $Y = G(X_1, X_2, \cdots, X_n)$ to calculate the actual value of the output response Y. When X_i takes each realized value, the cumulative influence of X_i on the probability density or probability distribution of Y is expressed as follows:

$$s(X_i) = \int_{-\infty}^{+\infty}\left|f_Y(y) - f_{Y|X_i}(y)\right|\mathrm{d}y, \tag{7}$$

where $s(X_i)$ is the shift between $f_Y(y)$ and $f_{Y|X_i(y)}$, and $f_Y(y)$ and $f_{Y|X_i(y)}$ are, respectively, the unconditional probability density function and the conditional probability density function of Y.

The moment-independent importance index δ_i is defined as follows:

$$\delta_i = \frac{1}{2}E_{X_i}[s(X_i)], \tag{8}$$

where $E_{X_i}[s(X_i)]$ is the expectation of $s(X_i)$, which can be obtained by

$$\begin{aligned} E_{X_i}[s(X_i)] &= \int_{-\infty}^{+\infty} f_{X_i}(x_i)s(X_i)\mathrm{d}x_i \\ &= \int_{-\infty}^{+\infty} f_{X_i}(x_i)\left[\int_{-\infty}^{+\infty}\left|f_Y(y) - f_{Y|X_i}(y)\right|\mathrm{d}y\right]\mathrm{d}x_i. \end{aligned} \tag{9}$$

It can be seen from equations (4) and (5) that the key to obtain δ_i is to determine $f_Y(y)$ and $f_{Y|X_i(y)}$ of Y, which is also the difficulty of moment-independent GSA. The kernel density estimation (KDE) method and orthogonal polynomial estimation (OPE) can directly fit the probability distribution according to the characteristics of the data samples themselves, and the accuracy is high, which are more representative methods among the nonparametric estimation methods.

The kernel density estimate of $f_Y(y)$ and $f_{Y|X_i(y)}$ can be expressed as follows:

$$\widehat{f}_Y(y) = \frac{1}{Nh}\sum_{i=1}^{N} K\left(\frac{y - y_i}{h}\right), \tag{10}$$

where $\widehat{f}_Y(y)$ is the kernel density estimation of $f_Y(y)$, h is the bandwidth parameter, N and y_i are, respectively, the sample size and function value of Y, and $K(\cdot)$ is the kernel density function, which needs to satisfy the following condition:

$$K(y) \geq 0, \int_{-\infty}^{+\infty} K(y)\mathrm{d}y = 1. \tag{11}$$

The Gaussian kernel function is adopted to estimate $\widehat{f}_Y(y)$ in this study, which is expressed as follows:

$$K\left(\frac{y - y_i}{h}\right) = \frac{1}{\sqrt{2\pi}}e^{-\left(\left(y - y_i/h\right)^2\right)/2}. \tag{12}$$

In order to avoid large errors caused by a single nonparametric estimation method, an orthogonal polynomial estimation method is introduced in this study. Considering that Hermite polynomial is simple and easy to implement, this study chooses it to approximate $f_Y(y)$. The main process is listed as follows: the probability density function $f(x)$ can be estimated by the expansion of the higher-order moment, which means $f(x)$ is nearly equal to the product of the orthogonal polynomial function and the weight function according to the principle of the Hermite orthogonal polynomial, which is expressed as follows:

$$\hat{f}(x) = \rho(x) \sum_{i=0}^{n} a_i H_i(x), \quad (13)$$

where $\rho(x) = (1/\sqrt{2\pi}\sigma)e^{[-((x-\mu)^2/2\sigma^2)]}$, μ and σ are the mean and standard deviation, respectively, a_i is the undetermined coefficient, which is determined by $a_i = \sum_{j=0}^{i} a_{ij} u_j(x)/h_i$, where a_{ij} is a constant, $u_j(x)$ is the j^{th} order central moment of the distribution function, and $h_i = 2^i i! \sqrt{\pi}$.

Then, $f_Y(y)$ is estimated by

$$\hat{f}_Y(Y) = \rho(y) \sum_{i=0}^{n} a_i H_i(y). \quad (14)$$

The calculation process of $f_{Y|X_i(y)}$ is similar to that of $f_Y(y)$.

Set δ_i^p as the moment-independent importance measure index of failure probability, which is expressed as follows [17]:

$$\begin{aligned} \delta_i^p &= \frac{1}{2} \mathrm{E}\left[\left| p_{fY} - p_{fY|X_i} \right| \right] \\ &= \frac{1}{2} \int_{-\infty}^{+\infty} \left| \int_F f_Y(y) \mathrm{d}y - \int_F f_{Y|X_i}(y) \mathrm{d}y \right| f_{X_i}(x_i) \mathrm{d}x_i \\ &= \frac{1}{2} \int_{-\infty}^{+\infty} \left| p_{fY} - p_{fY|X_i} \right| f_{X_i}(x_i) \mathrm{d}x_i, \end{aligned} \quad (15)$$

where $E(\cdot)$ is expectation; p_{fY} and $p_{fY|X_i}$ are, respectively, the unconditional failure probability and conditional failure probability of Y; $F = \{X\colon G(X) \le c_s\}$, in which X is the random variable and $X = (X_1, X_2, \ldots, X_n)$; $G(X)$ is the function of Y; c_s is a constant; and $f_{X_i}(x_i)$ is the probability density function of X_i.

Figure 1 shows the flowchart, and the function of Y needs to run $(n+1)N$ times to obtain the importance index, where n and N are the same as abovementioned.

3. Case Study

3.1. GSA of the Landslide Stability along PR303. The landslides caused by the Wenchuan earthquake are widely distributed in the southwest of China, and some of the landslide debris accumulates on the steep terrain, which is easily affected by external factors (such as aftershocks and rainfall infiltration) and leads to instability and damage again. For example, the landslides induced by the Wenchuan earthquake distributed from K1 to K18 of the province road (PR) 303 are prone to redestruction under the action of heavy rainfall (as shown in Figure 2(a)). With the help of site survey and GIS technology, 53 loose deposits landslides have been identified between K2 and K7 along PR303 (as shown in Figure 2(b)). These loose deposits landslides are considered as the representative instability slope. According to statistics, there were many landslides during the rainy season from 2009 to 2011, resulting in a large number of casualties and property losses. Tang and Zhang [18] predicted that slope failure would continue to occur in the next few years.

According to reference [18], the stability of the abovementioned landslides can be analyzed by the infinite slope model. The safety factor (Fs) of an infinite slope can be calculated by equation (13) as follows [19, 20]:

$$Fs = \frac{cL + N_t \tan\varphi}{(1-k_v)(W_n + W_{\text{sat}})\sin\xi + F_w + k_h(W_n + W_{\text{sat}})\cos\xi}, \quad (16)$$

where c and φ are, respectively, the cohesion and internal friction angle; L and ξ are the length of a slice and the slope angle, respectively; k_v and k_h are, respectively, the vertical and horizontal seismic acceleration coefficients; F_w and N_t are, respectively, the seepage force and the normal force on the sliding surface; W_{sat} and W_n are, respectively, the saturated zone and the weights of slices associated with the natural zone, and these forces are expressed as follows: $W_n = \gamma L(H-h)\cos\xi$, $W_{\text{sat}} = \gamma_{\text{sat}} Lh\cos\xi$, $N_t = (1 \pm k_v)(W_n + W_{\text{sat}})\cos\xi - k_h(W_n + W_{\text{sat}})\sin\xi$ and $F_w = \gamma_w Lh \sin\xi\cos\xi$, where H and h are, respectively, the thicknesses of the whole soil and saturated part of the soil, and $h = \text{m}H$ (m is the saturation index); and γ_n, γ_{sat}, and γ_w are, respectively, the natural unit weight, saturated unit weight of soil, and the unit weight of water.

In order to evaluate the influence of the parameters on the stability of the abovementioned loose deposit landslides, c, φ, γ, γ_{sat}, k_h, k_v, ξ, H, and m are taken as random variables for GSA in this study. There are 53 statistical data for γ, γ_{sat}, ξ, and H according to reference [18]. γ and γ_{sat} follow lognormal distribution, and ξ and H follow normal distribution based on the statistical analysis of these data. There is no statistical data for random variable c, φ, m, k_h, and k_v. Only the mean value of c and φ are known. The probability density distributions of c and φ are considered to follow normal or lognormal distributions [21, 22]. Wang et al. [23] suggested that the lognormal distribution is more suitable for simulating c and φ because of their physical meaning. Hence, c and φ are considered to follow the lognormal distribution in this case study. According to Li et al. [24], the negative correlation between c and φ varies from −0.20 to −0.92 based on the statistical information. Due to the lack of experimental data, the negative correlation coefficient between c and φ is assumed to be −0.5 in this case study. For m, k_h, and k_v, they vary equally between [0, 1], [0.1, 0.6], and [0.05, 0.45], respectively, according to reference [20], so this paper assumes that they all follow uniform distribution. In summary, the statistical information of random variables is shown in Table 1. Other parameter values are as follows: $\gamma_W = 9.81\ \text{kN/m}^3$ and the sample size $N = 1 \times 10^3$.

Taking Fs as the output response, the importance index of the nine random variables calculated by MC, LARS, KDE, and OPE are shown in Figure 3. It can be seen from Figure 3(a) that the importance indexes of ξ, k_h, and m are much larger than other random variables, which means that ξ and k_h have a greater impact on the stability of the loose deposit landslides when the correlation between c and φ is ignored. The importance indices of m and φ are slightly smaller than ξ and k_h, which indicates that their influence on slope stability is also very important. The importance indices

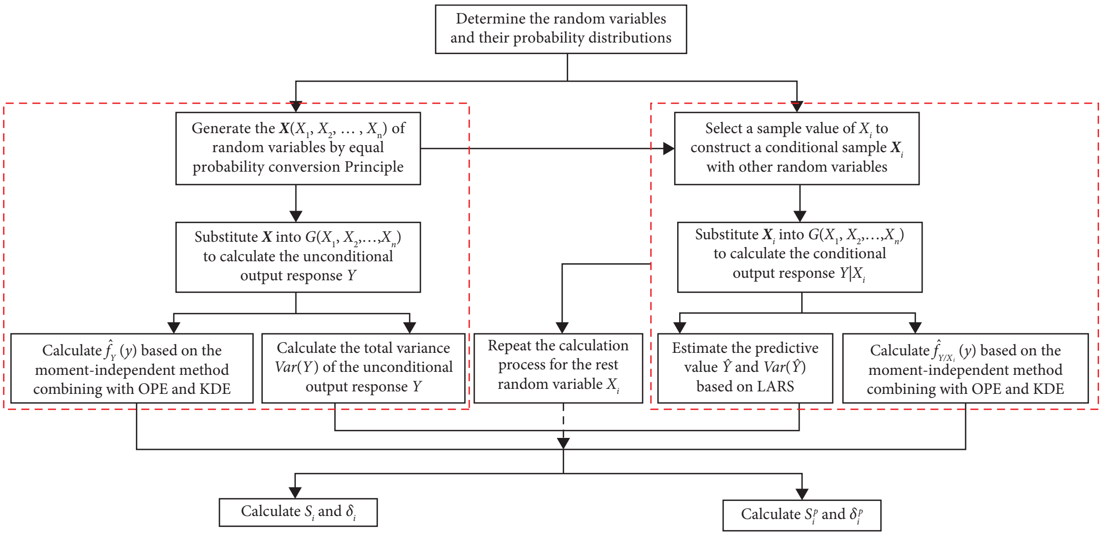

Figure 1: Calculation process of the importance index.

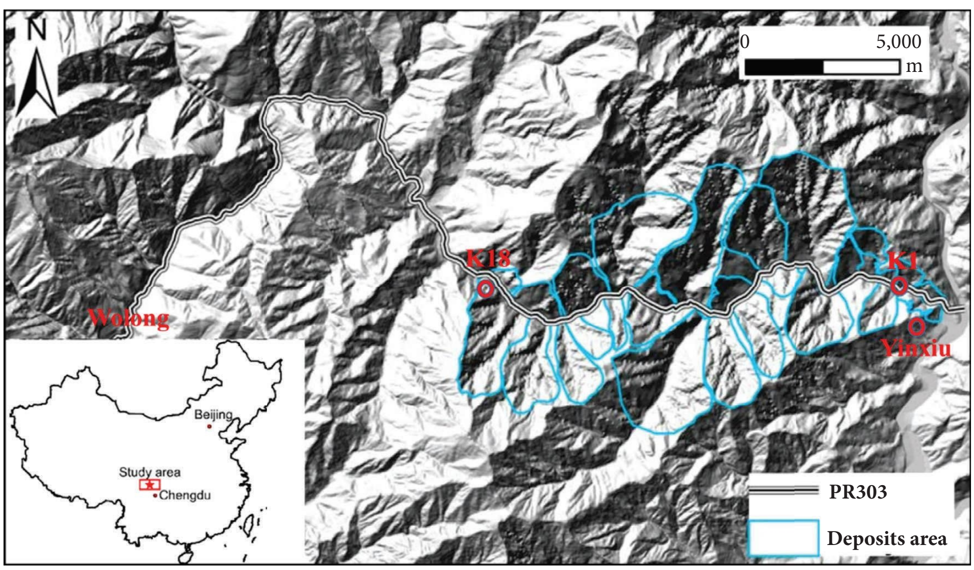

(a)

Figure 2: Continued.

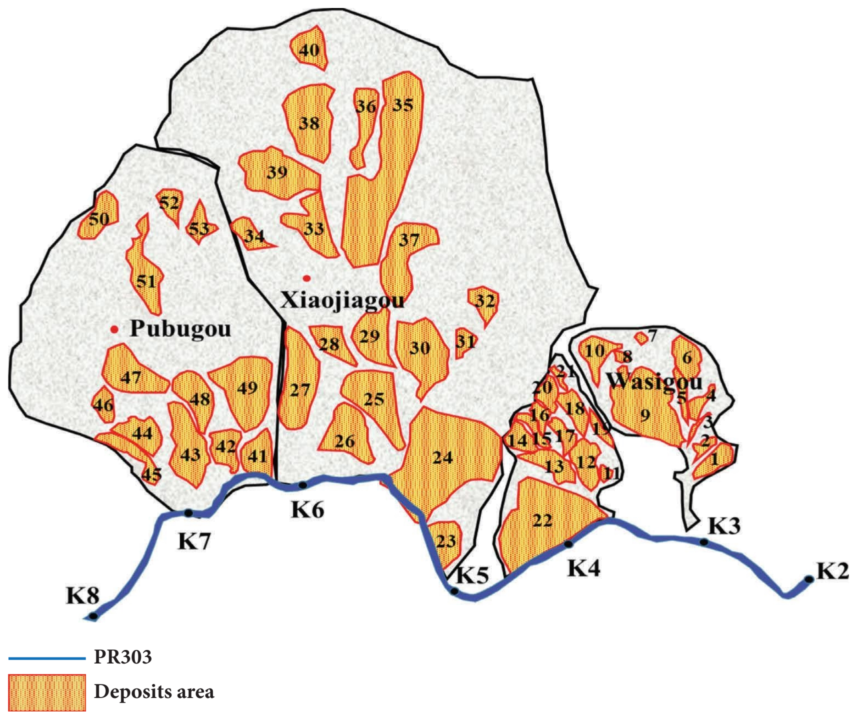

(b)

Figure 2: Landslides along PR303: (a) landslides between K1 and K18 and (b) loose deposits landslides between K2 and K7 [18].

Table 1: Random variables of the loose deposits landslides.

Random variables	Distribution	Probability density function (PDF)	Statistical information	Unit
c	Lognormal	$f(x) = (1/qx\sqrt{2\pi})\exp[-((\ln x - p)^2/2q^2)]$	$\mu = 8, \sigma = 2.56$	kPa
φ			$\mu = 32.7, \sigma = 4.578$	°
γ		$\mu = \exp(p + 0.5q^2)$,	$\mu = 17, \sigma = 1.7$	kN/m^3
γ_{sat}		$\sigma^2 = [\exp(q^2) - 1] \times \exp(2p + q^2)$	$\mu = 22, \sigma = 2.2$	kN/m^3
ξ	Normal	$f(x) = (1/\sqrt{2\pi}\sigma)\exp(-(x-\mu)^2/2\sigma^2)$	$\mu = 27.4, \sigma = 7.69$	°
H			$\mu = 374.72, \sigma = 161.11$	m
m	Uniform	$f(x) = \begin{cases} 1/(b-a), & a < x < b \\ 0, & \text{other} \end{cases}$	$[a, b] = [0, 1]$	—
k_h			$[a, b] = [0.1, 0.6]$	—
k_v			$[a, b] = [0.05, 0.45]$	—

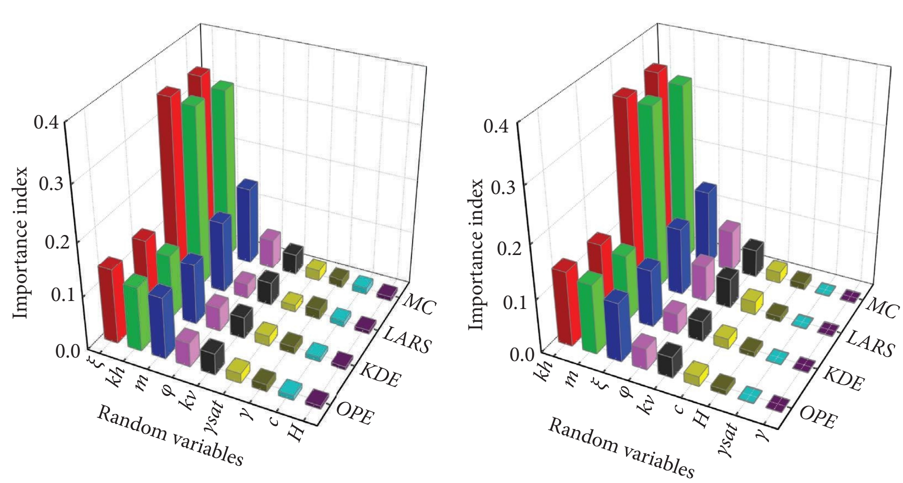

(a) (b)

Figure 3: Importance indices of random variables for the loose deposits landslides along PR303: (a) c and φ are independent and (b) c and φ are negatively correlated.

of c and H are small, which means that c and H have little impact on the stability of these landslides. The orders of the importance index calculated by MC, LARS, KDE, and OPE are $\xi > k_h > m > \varphi > k_v > \gamma_{sat} > \gamma > c > H$, $\xi > k_h > m > k_v > \varphi > \gamma > \gamma_{sat} > c > H$, $\xi > k_h > m > \varphi > k_v > \gamma_{sat} > \gamma > H > c$ and $\xi > k_h > m > \varphi > k_v > \gamma_{sat} > \gamma > c > H$, respectively.

As shown in Figure 3(a), the importance index calculated by MC and LARS are very close, and the importance orders are basically the same, which means the accuracy and validity of LARS have been verified. The values of the importance index obtained by KDE and OPE are different from those obtained by MC and LARS because the calculation principle of the variance-based GSA is different from that of the moment independence-based GSA. However, the importance orders calculated by KDE and OPE are almost exactly identical to that of MC. It is pointed out that if the importance orders calculated by other methods are the same as or similar to that of the variance-based MC method, then the results of these methods are accurate and reliable [25]. Therefore, the accuracy and validity of KDE and OPE have also been verified in this study.

It can be seen from Figure 3(b) that k_h and m have a greater impact on the stability of the loose deposit landslides when c and φ are negatively correlated, then followed by ξ, φ, k_v, and c, while H, γ_{sat}, and γ have little impact. The orders of the importance index calculated by MC, LARS, KDE, and OPE are $k_h > m > \xi > \varphi > k_v > c > H > \gamma_{sat} > \gamma$, $k_h > m > \xi > \varphi > k_v > c > \gamma_{sat} > H > \gamma$, $k_h > m > \xi > \varphi > k_v > c > \gamma_{sat} > \gamma > H$ and $k_h > m > \xi > \varphi > k_v > c > \gamma_{sat} > \gamma > H$, respectively. The importance orders of the nine random variables obtained by these four methods are basically the same, which also indicates that the accuracy and validity of the proposed methods are verified.

Comparing Figure 3(a) and 3(b), when c and φ are independent, the importance orders are significantly different from that of when c and φ are negatively correlated. For example, the importance order obtained by MC when c and φ are independent is $\xi > k_h > m > \varphi > k_v > \gamma_{sat} > \gamma > c > H$, while it is $k_h > m > \xi > \varphi > k_v > c > H > \gamma_{sat} > \gamma$ when c and φ are negatively correlated. Similar results were obtained by the other three methods. Therefore, it can be derived from this that the correlation between c and φ will have an important influence on the importance index, which cannot be ignored in the sensitivity analysis of slope stability.

3.2. GSA of the Typical Section of Xiaolangdi Dam. The Xiaolangdi Dam is an earth-rock dam with a loam inclined core wall. The elevation of the dam crest is 281m, and the normal water storage level of the reservoir is 275 m. The dam crest is 1,667 m long, and the dam bottom width is 864 m. The dam site is mainly composed of calcareous siliceous sandstone and calcareous cementitious sandstone. The base layer of the dam is composed of sandy pebble and bedrock from top to bottom, and the deepest part of sandy pebble overburden can reach 80 m. The core wall of the dam is made of clay, and both sides of the core wall are filled with enrockment. The antiseepage material of the inclined core wall is mainly composed of silty clay, and a high plastic soil zone is set at the top of the antiseepage wall.

As shown in Figure 4, the inclined wall (the clay area) has an important role in Xiaolangdi Dam. Considering that the D0 + 387.50 section is the largest one in the Xiaolangdi Dam, so it is very meaningful to perform the stability analysis in this study. According to Xu et al. [11], *Fs* can be obtained by the following equation set:

$$\begin{cases} F_1(\alpha, \beta, F_s, t) = \sum M_x = 0, \\ F_2(\alpha, \beta, F_s, t) = \sum M_y = 0, \\ F_3(\alpha, \beta, F_s, t) = \sum M_z = 0, \end{cases} \quad (17)$$

where α and β are the inclinations of intercolumn forces; M_x, M_y, and M_z are, respectively, the moments along the x, y, and z axes; and t is any time within the seismic wave period. For more details of the equations and the solution process, please refer to Zhou and Cheng [26] and Xu et al. [11].

For simplifying the calculation, c, φ, k_h, t, and f are considered as random variables in this case study, where f is the amplification factor. Other symbols have the same meaning as above. The experimental data of c and φ are obtained by the consolidated-undrained triaxial compression test, and both c and φ follow normal distribution [27, 28]. In addition, the correlation coefficient between c and φ is −0.544. Other random variables, k_h, t, and f, are assumed to follow a uniform distribution which is similar to those of case study 1. The information of these five random variables is listed in Table 2.

Figure 5(a) shows that among the 5 random variables, the random variable φ has the greatest impact on the stability of section D0 + 387.50 slope, while f has the least impact when the correlation between c and φ is ignored. The importance orders obtained by MC, LARS, KDE, and OPE are consistent, which are $\varphi > t > c > k_h > f$. Therefore, the results calculated by LARS, KDE, and OPE are accurate. As shown in Figure 5(b), when c and φ are negatively correlated, the importance orders obtained by MC, LARS, KDE, and OPE are consistent, which are $\varphi > t > k_h > c > f$. It is worth noting that the value of the importance index of the 5 random variables are significantly different when the relationship between c and φ are different, and the importance orders are also different. Therefore, the correlation of c and φ takes an important role in stability analysis of the section D0 + 387.50 slope.

3.3. GSA of the Highway Rock Slope. According to Chen [29], the highway slope is a homogeneous rock slope whose failure mode is plane shear sliding failure. The slope height and slope angle are, respectively, 150 m and 45°, and the shear strength parameters c and φ are 20 kPa and 20°. The rock mass density is 27 kN/m³. Then, *Fs* is expressed as follows [30]:

$$Fs = \frac{\gamma \tan\varphi H x_0 (x_0 - \cot\xi) + 2c\left(H^2 + x_0^2\right)}{\gamma H^2 (x_0 - H\cot\xi)}, \quad (18)$$

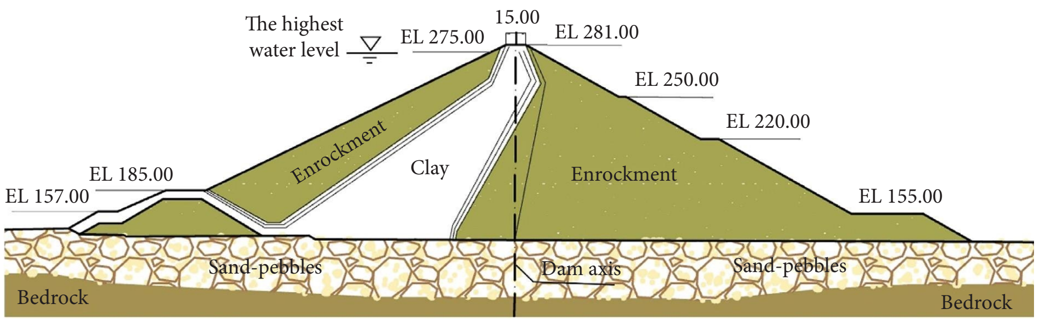

Figure 4: D0 + 387.50 section diagram of the Xiaolangdi dam [11] (EL unit: m).

Table 2: Random variables of the typical section D0 + 387.50 slope.

Random variables	Distribution	PDF	Parameters	Unit
c	Normal	$f(x) = 1/\sqrt{2\pi}\sigma \exp(-(x-\mu)^2/2\sigma^2)$	$\mu = 66.48, \sigma = 28.59$	kPa
φ			$\mu = 21.99, \sigma = 3.30$	°
k_h	Uniform	$f(x) = \begin{cases} 1/(b-a), & a < x < b \\ 0, & \text{other} \end{cases}$	$[a, b] = [0.1, 0.6]$	—
t			$[a, b] = [0, 0.2]$	s
f			$[a, b] = [1, 2]$	—

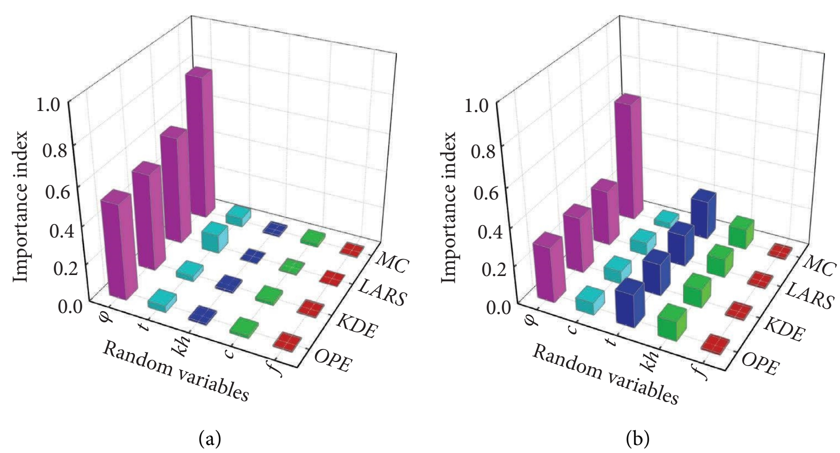

Figure 5: Importance indices of random variables for the section D0 + 387.50: (a) c and φ are independent and (b) c and φ are negatively correlated.

where x_0 is the projection of the starting point of the slipping surface on the abscissa, and H is the height of the slope. Other symbols have the same meanings as above.

The parameters c, φ, γ, H, and ξ are taken as the random variables for this case study, but there is no experiment data of them. Only the mean value of c and φ are known. As abovementioned in case study 1, c and φ are considered to follow the lognormal distribution, and the correlation coefficient between c and φ is assumed to be −0.5. The probability distributions of H and ξ are rarely reported, while their influence on slope stability should not be neglected. It is generally assumed that they vary equally within a certain interval; therefore, H and ξ are assumed to follow a uniform distribution. Therefore, the statistical information of the five random variables is listed in Table 3. The importance analysis results obtained by MC, LARS, KDE, and OPE are shown in Figure 6.

As shown in Figure 6, the importance index of each variable obtained by LARS algorithm is close to that of MC algorithm, which shows that LARS algorithm is effective. The value of the importance index of each variable calculated by KDE and OPE are nearly consistent, while different from those calculated by MC and LARS. The reason has been expressed in the abovementioned case study, so it will not be repeated here. It can be clearly seen from Figure 6(a) that the importance index value of ξ is obviously the largest and then followed by φ. The importance index of c and H is relatively small, and it is the smallest for γ. The importance orders obtained by MC, LARS, KDE, and OPE are the same, which is $\xi > \varphi > H > c > \gamma$. Therefore, the accuracy of KDE and OPE have also been verified.

When c and φ are negatively correlated, as shown in Figure 6(b), the importance orders obtained by MC, LARS, KDE, and OPE are consistent, which are $\xi > \varphi > c > H > \gamma$.

Table 3: Random variables of the expressway rock slope.

Random variables	Distribution	PDF	Parameters	Unit
c	Lognormal	$f(x) = (1/qx\sqrt{2\pi})\exp[-((\ln x - p)^2/2q^2)]$	$\mu = 20,\ \sigma = 6$	kPa
φ		$\mu = \exp(p + 0.5q^2)$,	$\mu = 20,\ \sigma = 4$	°
γ		$\sigma^2 = [\exp(q^2) - 1] \times \exp(2p + q^2)$	$\mu = 27,\ \sigma = 2.7$	kN/m^3
H	Uniform	$f(x) = \begin{cases} 1/(b-a), & a < x < b \\ 0, & \text{other} \end{cases}$	$[a, b] = [50, 250]$	m
ξ			$[a, b] = [15, 75]$	°

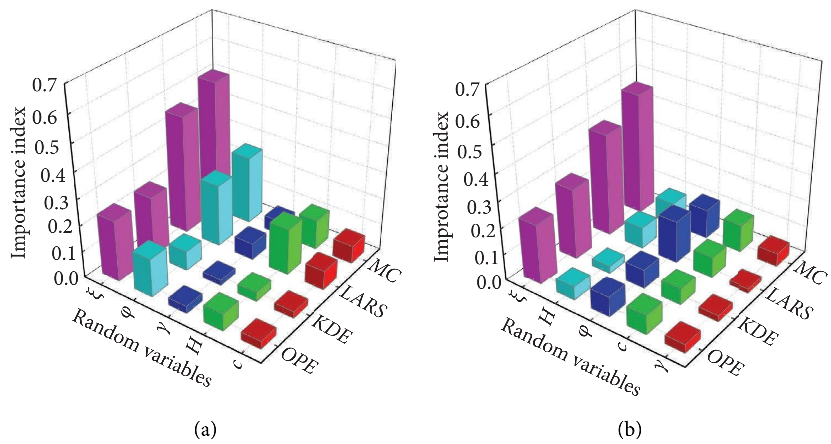

Figure 6: Importance indices of random variables for the expressway rock slope: (a) c and φ are independent and (b) c and φ are negatively correlated.

Compared to Figure 6(a) and 6(b), the importance orders are different when the relationship between c and φ are different. Therefore, the correlation between c and φ has important influence on slope stability, which should not be neglected.

4. Global Sensitivity Analysis Based on Failure Probability (p_f)

Take p_f as the output response; p_f is defined as $p_f = \text{Nu}/N$, where Nu is the number of $Fs < F$, F is the critical value of Fs, and N is the total number of Fs. The slope stability analysis model of case study 1 and 2 are relatively simple, so Nu is set to 1 as usual. Nu in Case 2 is set to 1.2 according to Yu [27]. Then, the results obtained by MC, LARS, KDE, and OPE are shown in Figures 7–9, respectively.

It can be seen from Figure 7(a) that when c and φ are independent, the importance orders based on failure probability obtained by MC, LARS, KDE, and OPE are $\xi > k_h > \varphi > m > k_v > \gamma_{sat} > \gamma > c > H$, $\xi > k_h > m > \varphi > k_v > \gamma_{sat} > c > \gamma > H$, $\xi > k_h > \varphi > m > k_v > \gamma > \gamma_{sat} > c > H$ and $\xi > k_h > \varphi > m > k_v > \gamma > c > \gamma_{sat} > H$, respectively. Obviously, the importance orders of failure probability obtained by the four methods are not completely the same. However, only c, γ, and γ_{sat} are different, and the orders of the three variables are ranked lower. In addition, the importance index values of c, γ, and γ_{sat} are very close. Therefore, the results of GSA based on failure probability obtained by these four methods are still effective and accurate.

When c and φ are negatively correlated, the importance orders of the random variables based on failure probability calculated by MC, LARS, KDE, and OPE are $k_h > m > \xi > \varphi > k_v > c > H > \gamma_{sat} > \gamma$, $k_h > m > \xi > \varphi > k_v > c > \gamma_{sat} > H > \gamma$, $k_h > m > \xi > k_v > \varphi > c > H > \gamma_{sat} > \gamma$ and $k_h > m > \xi > k_v > \varphi > c > H > \gamma_{sat} > \gamma$, respectively. It is clear that the importance orders of failure probability obtained by the four methods are not completely consistent. However, only the last three ranking γ, γ_{sat}, and H are different, and their importance index values are very close, which are all close to 0. Therefore, the results of GSA based on failure probability calculated by these four methods are still effective and accurate.

Compared with Figure 7(a) and 7(b), when c and φ are independent, the influence of ξ on the failure probability is the largest, and H has the smallest influence on the failure probability; while when c and φ are negatively correlated, k_h has the greatest impact on the failure probability and γ or H has the least effect on the failure probability. The correlation between c and φ must be given more attention when studying the impact of the uncertainty of random variables on the p_f for the loose deposits landslides along PR303.

As shown in Figure 8(a), the impact of random variables' uncertainty on p_f is obviously different. When c and φ are independent, the importance orders obtained by the four methods are, respectively, $\varphi > t > k_h > c > f$, $\varphi > k_h > t > c > f$, $\varphi > t > c > k_h > f$ and $\varphi > t > c > k_h > f$. Although the importance orders are not exactly the same, the greatest impact on the failure probability is always φ, and the smallest is f. When c and φ are negatively correlated, the importance orders obtained by the four methods are, respectively, $\varphi > c > t > k_h > f$, $\varphi > c > t > k_h > f$, $\varphi > c > t > f > k_h$ and

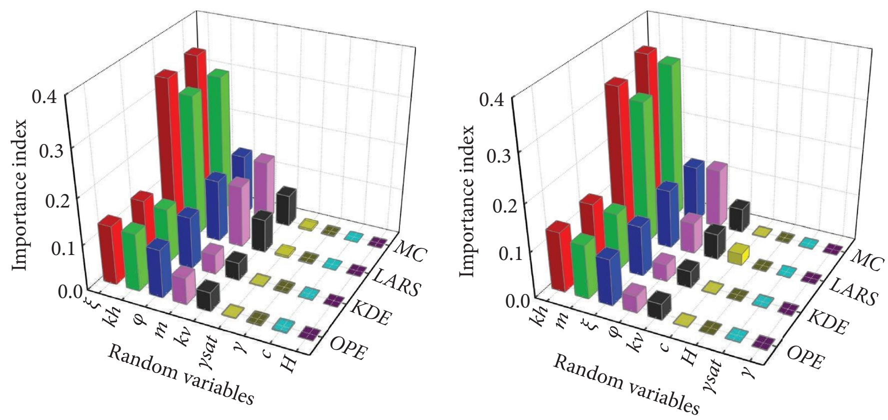

(a) (b)

FIGURE 7: Importance indices of the loose deposits landslides along PR303: (a) c and φ are independent and (b) c and φ are negatively correlated.

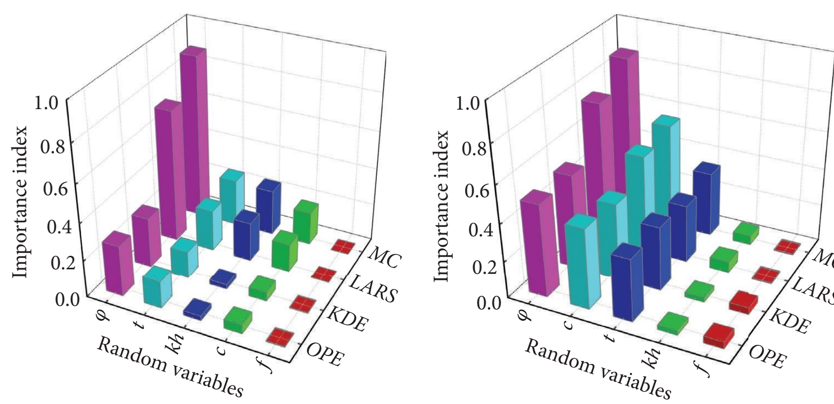

(a) (b)

FIGURE 8: Importance indices of the section D0 + 387.50: (a) c and φ are independent and (b) c and φ are negatively correlated.

$\varphi > c > t > f > k_h$ (shown in Figure 8(b)). Obviously, the importance orders of the random variables are different when the relationship between c and φ are different for the slope of the section D0 + 387.50.

The influence of the uncertainty of the random variables on the expressway rock slope is shown in Figure 9. When c and φ are independent, the importance orders obtained by MC and LARS are consistent and those obtained by KDE and OPE are the same, while there are some differences between MC and KDE, i.e., the importance orders are $\xi > \varphi > \gamma > H > c$, $\xi > \gamma > \varphi > H > c$, $\xi > \varphi > H > c > \gamma$ and $\xi > \varphi > H > c > \gamma$, respectively. In general, ξ and φ have more impact on p_f, while H, c, and γ have less impact on p_f. As shown in Figure 9(b), when c and φ are negatively correlated, the importance orders are $\xi > H > \varphi > c > \gamma$, $\xi > \varphi > c > H > \gamma$, $\xi > \varphi > H > c > \gamma$ and $\xi > \varphi > H > c > \gamma$, respectively. Compared to Figure 9(a) and 9(b), the importance orders obtained by the four methods still have some differences when the relationship between c and φ are different for the rock slope of expressway.

5. Discussion

In order to compare the differences in the influence of the uncertainty of random variables on Fs and p_f, the importance orders of each random variable to Fs and p_f are, respectively, listed in Tables 4 and 5.

As shown in Table 4, the importance ranking of the cumulative influence of each variable on Fs and p_f is not exactly the same. For the loose accumulation landslides along PR303 (case study 1), when c and φ are independent, the importance orders based on Fs and p_f obtained by MC are, respectively, $\xi > k_h > m > \varphi > k_v > \gamma_{\text{sat}} > \gamma > c > H$ and $\xi > k_h > \varphi > m > k_v > \gamma_{\text{sat}} > \gamma > c > H$. Where those are, respectively, $\xi > k_h > m > k_v > \varphi > \gamma > \gamma_{\text{sat}} > c > H$ and $\xi > k_h > m > \varphi > k_v > \gamma_{\text{sat}} > c > \gamma > H$ obtained by LARS $\xi > k_h > m > \varphi > k_v > \gamma_{\text{sat}} > \gamma > H > c$ and $\xi > k_h > \varphi > m > k_v > \gamma > \gamma_{\text{sat}} > c > H$ obtained by KDE, $\xi > k_h > m > \varphi > k_v > \gamma_{\text{sat}} > \gamma > c > H$ and $\xi > k_h > \varphi > m > k_v > \gamma > c > \gamma_{\text{sat}} > H$ obtained by OPE. Obviously, the importance ranking of each variable based on p_f is different from that based on Fs. Thus,

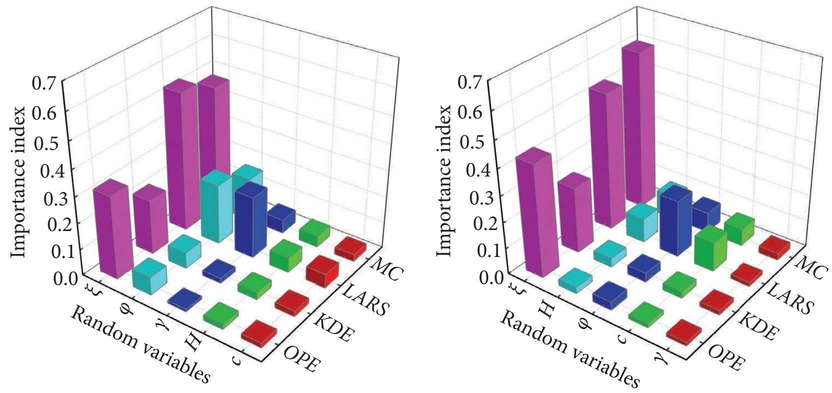

(a) (b)

FIGURE 9: Importance indices of the expressway rock slope: (a) c and φ are independent and (b) c and φ are negatively correlated.

TABLE 4: Ranking of the influence of random variables on Fs and p_f when c and φ are independent.

Methods	c and φ are independent		Case study
	Fs	p_f	
MC	$\xi > k_h > m > \varphi > k_v > \gamma_{sat} > \gamma > c > H$	$\xi > k_h > \varphi > m > k_v > \gamma_{sat} > \gamma > c > H$	Case study 1
LARS	$\xi > k_h > m > k_v > \varphi > \gamma > \gamma_{sat} > c > H$	$\xi > k_h > m > \varphi > k_v > \gamma_{sat} > c > \gamma > H$	
KDE	$\xi > k_h > m > \varphi > k_v > \gamma_{sat} > \gamma > H > c$	$\xi > k_h > \varphi > m > k_v > \gamma > \gamma_{sat} > c > H$	
OPE	$\xi > k_h > m > \varphi > k_v > \gamma_{sat} > \gamma > c > H$	$\xi > k_h > \varphi > m > k_v > \gamma > c > \gamma_{sat} > H$	
MC	$\varphi > t > c > k_h > f$	$\varphi > t > k_h > c > f$	Case study 2
LARS	$\varphi > t > c > k_h > f$	$\varphi > k_h > t > c > f$	
KDE	$\varphi > t > c > k_h > f$	$\varphi > t > c > k_h > f$	
OPE	$\varphi > t > c > k_h > f$	$\varphi > t > c > k_h > f$	
MC	$\xi > \varphi > H > c > \gamma$	$\xi > \varphi > \gamma > H > c$	Case study 3
LARS	$\xi > \varphi > H > c > \gamma$	$\xi > \gamma > \varphi > H > c$	
KDE	$\xi > \varphi > H > c > \gamma$	$\xi > \varphi > H > c > \gamma$	
OPE	$\xi > \varphi > H > c > \gamma$	$\xi > \varphi > H > c > \gamma$	

TABLE 5: Ranking of the influence of random variables on Fs and p_f when c and φ are negatively correlated.

Methods	c and φ are negatively correlated		Case study
	Fs	p_f	
MC	$k_h > m > \xi > \varphi > k_v > c > H > \gamma_{sat} > \gamma$	$k_h > m > \xi > \varphi > k_v > c > H > \gamma_{sat} > \gamma$	Case study 1
LARS	$k_h > m > \xi > \varphi > k_v > c > \gamma_{sat} > H > \gamma$	$k_h > m > \xi > \varphi > k_v > c > \gamma_{sat} > H > \gamma$	
KDE	$k_h > m > \xi > \varphi > k_v > c > \gamma_{sat} > \gamma > H$	$k_h > m > \xi > k_v > \varphi > c > H > \gamma_{sat} > \gamma$	
OPE	$k_h > m > \xi > \varphi > k_v > c > \gamma_{sat} > \gamma > H$	$k_h > m > \xi > k_v > \varphi > c > H > \gamma_{sat} > \gamma$	
MC	$\varphi > t > k_h > c > f$	$\varphi > c > t > k_h > f$	Case study 2
LARS	$\varphi > t > k_h > c > f$	$\varphi > c > t > k_h > f$	
KDE	$\varphi > t > k_h > c > f$	$\varphi > c > t > f > k_h$	
OPE	$\varphi > t > k_h > c > f$	$\varphi > c > t > f > k_h$	
MC	$\xi > \varphi > c > H > \gamma$	$\xi > H > \varphi > c > \gamma$	Case study 3
LARS	$\xi > \varphi > c > H > \gamma$	$\xi > \varphi > c > H > \gamma$	
KDE	$\xi > \varphi > c > H > \gamma$	$\xi > \varphi > H > c > \gamma$	
OPE	$\xi > \varphi > c > H > \gamma$	$\xi > \varphi > H > c > \gamma$	

the influence of the same variable on the importance of Fs and p_f is not consistent.

For the Xiaolangdi Dam slope, when c and φ are independent, the importance orders based on Fs obtained by the four methods are consistent, which are $\varphi > t > c > k_h > f$, while those are $\varphi > t > k_h > c > f$ (obtained by MC), $\varphi > k_h > t > c > f$ (obtained by LARS), and $\varphi > t > c > k_h > f$ (obtained by KDE and OPE) based on p_f. For the expressway rock slope, when c and φ are independent, the importance orders based on Fs obtained by the four methods are consistent, which are $\xi > \varphi > H > c > \gamma$, while those are, respectively, $\xi > \varphi > \gamma > H > c$, $\xi > \gamma > \varphi > H > c$, $\xi > \varphi > H$

$> c > \gamma$ and $\xi > \varphi > H > c > \gamma$ based on p_f. The results of these two case studies indicate that the influence of the random variable on Fs and p_f is different.

As shown in Table 5, when c and φ are negatively correlated, the importance orders based on Fs and p_f obtained by MC and LARS are consistent, while those are different obtained by KDE and OPE for the case study 1. Specifically, the orders based on Fs and p_f obtained by KDE are, respectively, $k_h > m > \xi > \varphi > k_v > c > \gamma_{\text{sat}} > \gamma > H$ and $k_h > m > \xi > k_v > \varphi > c > H > \gamma_{\text{sat}} > \gamma$. The results of OPE are the same as KDE. It can be seen that the impact of the uncertainty of each random variable on Fs and p_f are different for the loose deposits landslides along PR303.

For case study 2, the importance orders for Fs and p_f are also different. For example, the importance orders for Fs obtained by the four methods are consistent, which is $\varphi > t > k_h > c > f$, while those are $\varphi > c > t > k_h > f$ (obtained by MC and LARS), $\varphi > c > t > f > k_h$ (obtained by KDE and OPE) when c and φ are negatively correlated. Therefore, it can be drawn that the influence of random variables on p_f and Fs is different for the slope of the section D0 + 387.50 slope of Xiaolangdi Dam.

For case study 3, the importance orders for Fs obtained by the four methods are consistent, which is $\xi > \varphi > c > H > \gamma$, while those are $\xi > H > \varphi > c > \gamma$ (obtained by MC), $\xi > \varphi > c > H > \gamma$ (obtained by LARS), and $\xi > \varphi > H > c > \gamma$ (obtained by KDE and OPE) when c and φ are negatively correlated. Therefore, it indicates that the influence of random variables on p_f and Fs is different for the slope of the expressway rock slope.

In summary, the influence of random variables on p_f and Fs is different whether the relationship between c and φ is considered or not. The results obtained by the other three methods have similar characteristics. Therefore, Fs should not be the only criterion for slope stability.

In addition, while comparing Tables 4 and 5, the importance orders of the random variables are different when the relationship between c and φ is different. For example, the importance order-based Fs obtained by MC is $\xi > k_h > m > \varphi > k_v > \gamma_{\text{sat}} > \gamma > c > H$ when c and φ are independent in case study 1, while it is $k_h > m > \xi > \varphi > k_v > c > H > \gamma_{\text{sat}} > \gamma$ when c and φ are negatively correlated. In case study 2, those are, respectively, $\varphi > \mathrm{t} > \mathrm{c} > k_h > \mathrm{f}$ and $\varphi > \mathrm{t} > k_h > \mathrm{c} > \mathrm{f}$ (obtained by MC). In case study 3, those are, respectively, $\xi > \varphi > \mathrm{H} > \mathrm{c} > \gamma$ and $\xi > \varphi > \mathrm{c} > \mathrm{H} > \gamma$ (obtained by MC). The results obtained by the other three methods are generally consistent, which shows that the relationship between c and φ will impact the importance of the random variables, and the correlation between c and φ should not be neglected.

It is pointed out that the probabilistic approaches which can integrate the Fs with advanced failure probability prediction have seen fast development in recent years. For example, Ji et al. [31] proposed a simplified iterative algorithm for forward/inverse first-order reliability method to perform the geotechnical reliability-based designs of a strip footing and an earth slope. Ji et al. [32] studied the seismic slope failure mechanism of a rotating sliding body to clarify the mechanism of slope movement triggered by earthquake and the criteria of seismic performance or failure state and proposed a reliability-based design of the allowable displacement method for slope stability analysis. Ji et al. [33] established a modified rotational sliding block model considering depth-dependent shear strength and dynamic yield acceleration, and investigated the influence of slope parameters on the failure probability of seismic slope. In order to improve the efficiency and accuracy of reliability analysis, Ji and Wang [34] developed a modified weighted uniform simulation method for reliability analysis involving nonnormal random variables by adopting Nataf transformation. This paper currently only analyzes the impact of parameter uncertainty on Fs and p_f. In the future, further research will be conducted on the impact of other reliability indicators of slope stability.

In addition, more and more computer technologies are used in slope risk assessment, such as machine learning, intelligent optimization algorithms, etc. For example, Ma et al. [35] developed an automated machine learning-based landslide susceptibility mapping (LSM), which provides a high performance solution for machine learning-based LSM. Liu et al. [36] proposed an earthworm optimization algorithm-optimized support vector regression to predict reservoir landslide displacement. Jia et al. [37] developed a multilevel, comprehensive method based on the analytic hierarchy process to evaluate the hazards of ground fissures. Long et al. [38] studied the landslide evolution in the worst-affected area (Mianyuan River Basin) based on supervised classification methods and multitemporal remote sensing images during the decade from 2007 to 2018. These techniques provide more efficient and more convenient methods for slope stability assessment. The follow-up work of this paper will try to introduce machine learning algorithm to analyze the influence of parameter uncertainty on reliability index, in order to provide a more practical method for landslide risk assessment.

6. Conclusions

In this paper, the variance-based methods (LARS and MC) and the moment-independent-based methods (KDE and OPE) are, respectively, used to study the impact of random variables on Fs and p_f. Three engineering cases have been applied to verify the accuracy and efficacy of those proposed methods. The results obtained by LARS, KDE, and OPE are in good sync with those calculated by the variance-based MC method, which is considered to be an exact solution and is often used to verify other methods. Therefore, the proposed methods are accurate and effective. When c and φ are independent or correlated, the influence of parameters on Fs and p_f are very different, and the importance orders are also obviously different, which indicates that the correlation between c and φ has a nonnegligible impact on the importance analysis for slope stability. The importance orders based on Fs and p_f differ greatly, which indicates that the influence of each random variable on Fs and p_f is different. The impact of variables with large value of the importance index should be emphatically considered in the risk assessment of slope stability. Fs should not be the only criterion in the uncertainty analysis.

Data Availability

The datasets used and/or analyzed during the current study are available from the corresponding author on reasonable request.

Conflicts of Interest

The authors declare that they have no conflicts of interest.

Acknowledgments

This work was supported by Suqian Sci & Tech Program (Grant nos. K202308 and K202142), Jiangsu Province Industry University Research Cooperation Project (no. BY20231207), Basic Science Research (Natural Science) of Colleges and Universities in Jiangsu Province (General Project, Grant no. 23KJB410002), and High-Level Talent Introduction Scientific Research Start-Up Project of Suqian University (Grant no. 2022XRC007 and Grant no. 2022XRC022).

References

[1] J. Jin, C. Yan, Y. Tang, and Y. Yin, "Mine geological environment monitoring and risk assessment in arid and semiarid areas," *Complexity*, vol. 2021, Article ID 3896130, 10 pages, 2021.

[2] J. Cai, T. C. J. Yeh, E. Yan, R. Tang, J. Wen, and S. Huang, "An adaptive sampling approach to reduce uncertainty in slope stability analysis," *Landslides*, vol. 15, no. 6, pp. 1193–1204, 2018.

[3] M. Abdulai and M. Sharifzadeh, "Uncertainty and reliability analysis of open pit rock slopes: a critical review of methods of analysis," *Geotechnical & Geological Engineering*, vol. 37, no. 3, pp. 1223–1247, 2019.

[4] H. Zhao and S. Li, "Determining geomechanical parameters and a deformation uncertainty analysis of the Longtan Hydropower Station slope, China," *Bulletin of Engineering Geology and the Environment*, vol. 80, no. 8, pp. 6429–6443, 2021.

[5] Z. Su, Y. Wang, and H. Zhang, "Deterministic and uncertainty analysis of a reservoir slope stability and failure mechanism under combined action of multi-hazards," *Geotechnical & Geological Engineering*, vol. 40, no. 4, pp. 2187–2199, 2022.

[6] Q. Ren and X. Meng, "Study on mechanical response and stability algorithm of soft and hard rock interbedded slope excavation," *Complexity*, vol. 2022, Article ID 3331097, 26 pages, 2022.

[7] F. Li and H. Zhang, "Stability evaluation of rock slope in hydraulic engineering based on improved support vector machine algorithm," *Complexity*, vol. 2021, Article ID 8516525, 13 pages, 2021.

[8] A. Alexanderian, P. A. Gremaud, and R. C. Smith, "Variance-based sensitivity analysis for time-dependent processes," *Reliability Engineering & System Safety*, vol. 196, 2020.

[9] A. Subramanian and S. Mahadevan, "Variance-based sensitivity analysis of dynamic systems with both input and model uncertainty," *Mechanical Systems and Signal Processing*, vol. 166, 2022.

[10] W. Yun, Z. Lu, K. Feng, and L. Li, "An elaborate algorithm for analyzing the Borgonovo moment-independent sensitivity by replacing the probability density function estimation with the probability estimation," *Reliability Engineering & System Safety*, vol. 189, pp. 99–108, 2019.

[11] Z. Xu, X. Zhou, and Q. Qian, "The uncertainty importance measure of slope stability based on the moment-independent method," *Stochastic Environmental Research and Risk Assessment*, vol. 34, no. 1, pp. 51–65, 2020.

[12] S. Khan, P. Kaklis, A. Serani, and M. Diez, "Geometric moment-dependent global sensitivity analysis without simulation data: application to ship hull form optimisation," *Computer-Aided Design*, vol. 151, 2022.

[13] B. Efron, T. Hastie, I. Johnstone, and R. Tibshirani, "Least angle regression," *Annals of Statistics*, vol. 32, no. 2, pp. 407–451, 2004.

[14] Z. Xu, X. Zhou, and Q. Qian, "The global sensitivity analysis of slope stability based on the Least Angle Regression," *Natural Hazards*, vol. 105, no. 3, pp. 2361–2379, 2021.

[15] I. Sobol, "Global sensitivity indices for nonlinear mathematical models and their Monte Carlo estimates," *Mathematics and Computers in Simulation*, vol. 55, no. 1-3, pp. 271–280, 2001.

[16] E. Borgonovo, "A new uncertainty importance measure," *Reliability Engineering & System Safety*, vol. 92, no. 6, pp. 771–784, 2007.

[17] L. Cui, Z. Lü, and X. Zhao, "Moment-independent importance measure of basic random variable and its probability density evolution solution," *Science China Technological Sciences*, vol. 53, no. 4, pp. 1138–1145, 2010.

[18] W. Tang and L. Zhang, "Development of a risk-based landslide warning system," *GeoRisk 2011*, vol. 224, pp. 25–49, 2011.

[19] H. Ghiassian and S. Ghareh, "Stability of sandy slopes under seepage conditions," *Landslides*, vol. 5, no. 4, pp. 397–406, 2008.

[20] X. Wu, "Development of fragility functions for slope instability analysis," *Landslides*, vol. 12, no. 1, pp. 165–175, 2015.

[21] D. C. Tobutt, "Monte Carlo simulation methods for slope stability," *Computers & Geosciences*, vol. 8, no. 2, pp. 199–208, 1982.

[22] G. A. Fenton and D. V. Griffiths, "Bearing capacity prediction of spatially random $c-\varphi$ soils," *Canadian Geotechnical Journal*, vol. 40, no. 1, pp. 54–65, 2003.

[23] Y. Wang, T. Y. Zhao, and Z. J. Cao, "Site-specific probability distribution of geotechnical properties," *Computers and Geotechnics*, vol. 70, pp. 159–168, 2015.

[24] D. Li, X. Tang, and C. Zhou, *The Uncertainty Representation and Reliability Analysis of Geotechnical Parameters Based on Copula Theory*, Science Press Beijing, Beijing, China, 2015.

[25] K. Zhang, Z. Lu, D. Wu, and Y. Zhang, "Analytical variance based global sensitivity analysis for models with correlated variables," *Applied Mathematical Modelling*, vol. 45, pp. 748–767, 2017.

[26] X. Zhou and H. Cheng, "Stability analysis of three-dimensional seismic landslides using the rigorous limit equilibrium method," *Engineering Geology*, vol. 174, pp. 87–102, 2014.

[27] Q. Yu, "*Research on the reliability of the stability of the earth-rock fill dam and its application*", M.S. thesis, Hohai University, Nanjing, China, 2006.

[28] L. Zhang, X. Tang, and D. Li, "Bivariate distribution model of soil shear strength parameter using copula," *Journal of Civil Engineering and Management*, vol. 30, no. 2, pp. 11–17, 2013.

[29] P. Chen, in *Study on the Stability and its Influence Factors for Highway Bedding Rock Slopes*, Zhejiang University, Hangzhou, China, 2012.

[30] E. Hoek and J. W. Bray, *Rock Slope Engineering*, Institution of Mining and Metallurgy, London, UK, 1981.

[31] J. Ji, C. S. Zhang, Y. F. Gao, and J. Kodikara, "Reliability-based design for geotechnical engineering: an inverse FORM approach for practice," *Computers and Geotechnics*, vol. 111, pp. 22–29, 2019.

[32] J. Ji, W. J. Zhang, F. Zhang, Y. F. Gao, and Q. Lü, "Reliability analysis on permanent displacement of earth slopes using the simplified Bishop method," *Computers and Geotechnics*, vol. 117, 2020.

[33] J. Ji, C. W. Wang, Y. F. Gao, and L. M. Zhang, "Probabilistic investigation of the seismic displacement of earth slopes under stochastic ground motion: a rotational sliding block analysis," *Canadian Geotechnical Journal*, vol. 58, no. 7, pp. 952–968, 2021.

[34] J. Ji and L. P. Wang, "Efficient geotechnical reliability analysis using weighted uniform simulation method involving correlated nonnormal random variables," *Journal of Engineering Mechanics*, vol. 148, no. 6, 2022.

[35] J. W. Ma, D. Z. Lei, Z. Y. Ren, C. H. Tan, D. Xia, and H. X. Guo, "Automated machine learning-based landslide susceptibility mapping for the three gorges reservoir area, China," *Mathematical Geosciences*, 2023.

[36] Z. Y. Liu, J. W. Ma, D. Xia et al., "Toward the reliable prediction of reservoir landslide displacement using earthworm optimization algorithm-optimized support vector regression (EOA-SVR)," *Natural Hazards*, vol. 120, no. 4, pp. 3165–3188, 2023.

[37] Z. j. Jia, J. B. Peng, Q. Z. Lu et al., "A comprehensive method for the risk assessment of ground fissures: case study of the eastern weihe basin," *Journal of Earth Sciences*, vol. 34, no. 6, pp. 1892–1907, 2023.

[38] Y. J. Long, W. L. Li, R. Q. Huang, Q. Xu, B. Yu, and G. Liu, "A comparative study of supervised classification methods for investigating landslide evolution in the mianyuan River Basin, China," *Journal of Earth Sciences*, vol. 34, no. 2, pp. 316–329, 2023.